
HiC2Self: Self-supervised Hi-C contact map denoising

Rui Yang **Alireza Karbalayghareh** **Christina Leslie**
Sloan Kettering Institute Sloan Kettering Institute Sloan Kettering Institute
ruiy4001@med.cornell.edu karbalaa@mskcc.org cleslie@cbio.mskcc.org

Abstract

1 We propose HiC2Self, a self-supervised method for denoising Hi-C contact maps
2 that needs only low coverage data for training and imputes high coverage interaction
3 count data that can be used for downstream analyses. Using a self-denoising
4 framework based on Noise2Self, we designed a unique mask structure tailored
5 for Hi-C contact maps and adopted a negative binomial loss function in order to
6 directly process the raw count matrix without additional normalization or recovery
7 steps. We found our self-supervised method was competitive with or outperformed
8 existing supervised Hi-C denoising algorithms while providing greater ease of use.

9 1 Introduction

10 Hi-C is a genome-wide chromatin conformation capture assay that is used to study 3D genomic
11 organization. Hi-C paired-end sequencing data produces a contact matrix between genomic bins
12 that reveals principles of chromatin folding at resolutions, such as A/B compartments when data
13 is binned at megabase scale and topologically associating domains (TADs) for 10-50kb bins (1).
14 Intra-chromosomal Hi-C contact maps are usually visualized by a symmetric heatmap, where x and
15 y coordinates indicate genomic locations along the chromosome, and each pixel shows the strength
16 of chromatin interaction (normalized read count) between the corresponding bins. High-resolution
17 Hi-C contact maps require generation of multiple replicate libraries and extremely high sequencing
18 coverage (1-2B reads), incurring considerable costs. Contact maps generated from libraries with only
19 shallow sequencing have high noise due to sparsity.

20 Given the success of deep learning technology for image denoising and super-resolution, several
21 groups have designed supervised deep learning models to "denoise" Hi-C contact maps. HiCPlus
22 (2) and HiCNN (3) use convolutional neural networks to predict high coverage 2D contact maps
23 from low coverage or downsampled contact maps in the same cell type. hicGAN (4), DeepHiC (5)
24 and HiCSR (6) all use generative adversarial networks (GAN) to impute high resolution data, with
25 DeepHiC and HiCSR employing loss functions specifically tailored to Hi-C data. These supervised
26 approaches all require paired low-/high-coverage Hi-C data to train the model, which can then be
27 applied to other cell types where only low-coverage data are available. Existing approaches also
28 normalize and preprocess Hi-C input data to fit the training framework, which typically requires an
29 additional post-prediction recovery procedure to reconstruct a genome-wide matrix for downstream
30 analysis.

31 In this study, we present HiC2Self, a self-supervised Hi-C denoising model that only requires
32 low-coverage Hi-C data for training and can be applied directly to raw count matrices without
33 normalization steps. The self-supervision framework is based on Noise2Self (7), with a mask
34 structure and negative-binomial loss function designed for Hi-C raw count matrices.

35 2 Method

36 **Data Preparation** High coverage Hi-C data sets are generated by sequencing multiple libraries and
37 aggregating read counts across libraries. To obtain low-coverage Hi-C training data, we generated a
38 contact map from a single library and evaluated performance against the aggregated multi-library
39 map. Intra-chromosomal Hi-C raw count contact maps were generated without normalization. For
40 each chromosome in the low-coverage dataset, we further extracted equal-sized square submatrices

41 along the diagonal, representing genomic interactions up to 1Mb in linear distance. These symmetric
 42 submatrices X are used as the training set for our model.

43 **Self-supervision framework** Noise2Self (7) is a self-supervised denoising framework that uses
 44 \mathcal{J} -invariant functions f , where \mathcal{J} represents a partition of the input data dimensions m into subsets,
 45 and we consider a subset $J \in \mathcal{J}$ and its complement J^C . Given an unseen clean signal $y \in \mathbb{R}^m$, we
 46 assume that x is a mean-zero noisy observation, where $\mathbb{E}[x|y] = y$. For any fixed subset J , we further
 47 assume that a noisy observation on subdimension x_J is independent of the one on its complement
 48 x_{J^C} given y . With these two assumptions, a function $f : \mathbb{R}^m \rightarrow \mathbb{R}^m$ is defined as \mathcal{J} -invariant if
 49 $f(x)_J$ is independent of x_J for every $J \in \mathcal{J}$.

50 The ordinary denoising loss function is defined as

$$\mathcal{L}_f = \mathbb{E}_{x,y} \|f(x) - y\|^2 = \mathbb{E}_x \|f(x) - x\|^2 + \|x - y\|^2 - 2\langle f(x) - x, x - y \rangle$$

51 which is the sum of a self-supervised loss and the variance of the noise. With a J -invariant function
 52 f and the previous assumptions, this simplifies to

$$\mathcal{L}(f) = \sum_{J \in \mathcal{J}} \mathbb{E} \|f_J(x_{J^C}) - x_J\|^2$$

53 so that the denoising function f can be optimized using only noisy observations x .

54 The \mathcal{J} -invariance property is realized using masks. We denote the masked area as x_J and the
 55 unmasked area as x_{J^C} . Given the symmetric nature of Hi-C contact maps and the requirement that
 56 $x_J \perp\!\!\!\perp x_{J^C} | y$, we designed masks that are symmetric with respect to the diagonal.

57 The training framework is shown in Figure 1A.

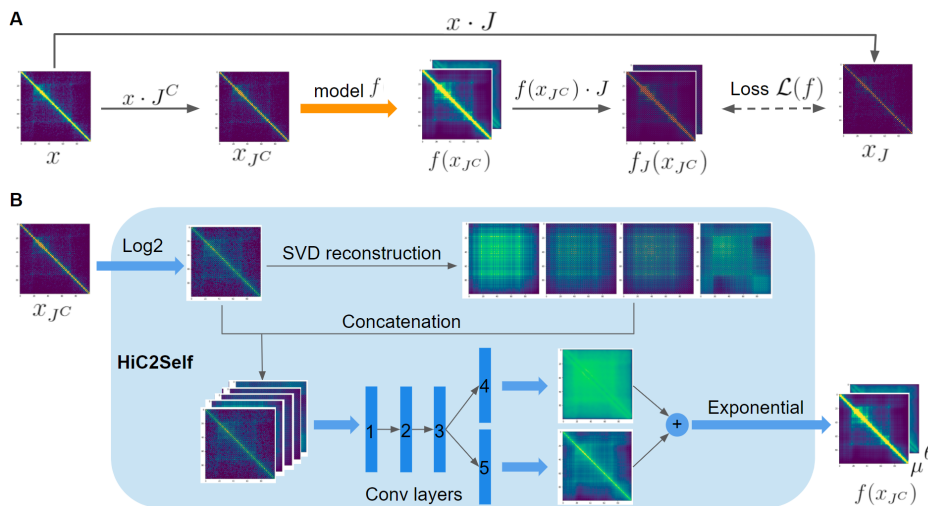


Figure 1: Training framework and model architecture

58 **Model architecture** HiC2Self uses a simple convolutional neural network (CNN), as shown in
 59 Figure 1B. Within the model, raw count input matrices X were first \log_2 -transformed ($X' =$
 60 $\log_2(X_{J^C} + 1)$) in order to guarantee numerical stability for subsequent steps.

61 Singular value decomposition (SVD) and low-rank reconstruction is a classic approach for 2D image
 62 compression and denoising. In order to enhance the signal extracted from low-coverage submatrices,
 63 we performed SVD on the \log_2 -transformed matrices $X' = U\Sigma U^T$, generated reconstructions
 64 $X'_k = \sum_{i=1}^k u_i \Sigma_i u_i^T$ using the top k eigenvectors, $k \in [1, 4]$, and concatenated these matrices
 65 with X' as additional input channels for the CNN.

66 The convolutional part of the model consists of five equal-sized convolutional layers, where each of
 67 the first three layers is followed by ReLU activation functions (see Table 1). An exponential function
 68 was used as the activation function for layer 4 and 5 in order to transform output values back into raw
 69 count space.

Layer	Type	Filter size	input dimension	output dimension	input channels	output channels	Activation function
1	Convolution	5×5	100×100	100×100	5	64	ReLU
2	Convolution	5×5	100×100	100×100	64	64	ReLU
3	Convolution	5×5	100×100	100×100	64	32	ReLU
4	Convolution	3×3	100×100	100×100	32	1	Exponential
5	Convolution	3×3	100×100	100×100	32	1	Exponential

Table 1: Structure of convolutional layers

Loss function Inspired by the deep count autoencoder (DCA) model for single cell data (8), we used a negative binomial loss for the raw count matrices to train our model. We assume that count from each bin (x_{ij}) of the contact map X follows a negative binomial distribution with parameters μ_{ij} and θ_{ij} , $x_{ij} \sim NB(\mu_{ij}, \theta_{ij})$. The loss function is defined as

$$\mathcal{L}(f) = -\log L_{NB} = \sum (\log \Gamma(x+1) + \log \Gamma(\theta) - \log \Gamma(x+\theta) + \theta \log(\frac{\mu+\theta}{\theta}) + x \log(\frac{\mu+\theta}{\mu}))$$

As shown in Figure 1B, HiC2Self outputs two channels, corresponding to μ and θ in the loss function above. We use μ_{ij} , the expected value for each bin x_{ij} , as the predicted value for our denoising results.

Genome-wide prediction HiC2Self produces denoised results as raw counts, which can easily be assembled into a whole-chromosome prediction. To do this, we extracted submatrices along the diagonal, consecutively striding by one bin each time. Denoised results were generated for each submatrix, and predicted counts for overlapping submatrices were averaged. The resulting predicted high coverage results were saved as a .hic file using Juicer tools (9) for downstream analysis.

3 Experiments and Results

Data HiC2Self was trained and evaluated on real low- and high-coverage Hi-C data as described above. Low-/high-coverage raw count matrices for the ENCODE GM12878 cell line were downloaded from GEO (GSE63525 (10)). A single low-coverage library (experiment HIC001) with 2.5M reads was used as low-coverage data to train the model, and pooled primary libraries with 3.5B reads (low/high ratio = 1/18) was used as high-coverage Hi-C data to evaluate model performance. Raw count data were downloaded in .hic format and further binned at 10kb resolution matrix using Juicer (9). Equal-sized (100×100) submatrices were extracted along the diagonal from intra-chromosomal low-coverage Hi-C contact maps to train the model.

Denoising on normalized data In order to validate our model framework and compare with previously published methods, we first trained our model (with necessary changes) using mean squared error on normalized data (log2-transformation followed by min/max rescaling to produce values between -1 and 1). The supervised model hicGAN was trained on 5,000 submatrices extracted from paired low-/high-coverage Hi-C data, with chromosome 3, 8, 12 held out for testing. We use Pearson correlation (per genomic distance) with high coverage data as the metric for evaluation and found comparable performance to hicGAN (Figure 2).

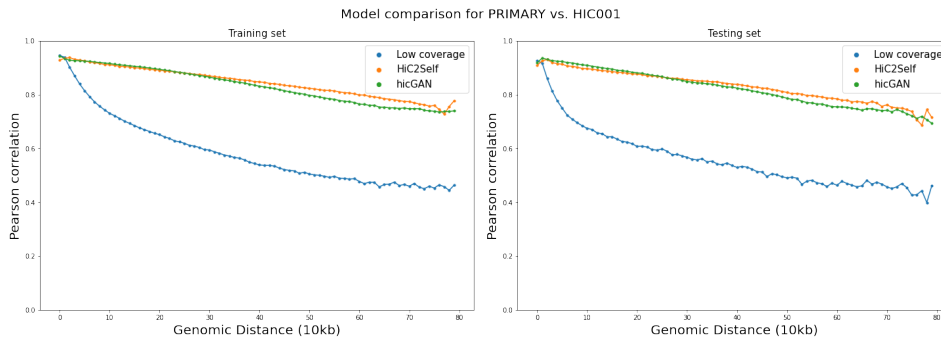


Figure 2: Performance on log-transformed data

94 **Whole chromosome prediction** Given the competitive performance on normalized data, we next
 95 trained our model with negative binomial loss on raw count data and produced predicted high coverage
 96 raw count contact maps. We generated denoised predictions within 1Mb distance from diagonal for
 97 chromosome 18 and multiplied by a scaling factor of 10 to increase the count range. The result was
 98 saved into .hic format and visualized using Juicebox (9) (Figure 3, color scale for the low-coverage
 99 matrix is 1/10 of the scale for denoised and high coverage matrices.)
 100 We again used Pearson correlation by genomic distance to evaluate model performance on log₂
 101 transformed counts. For comparison, we downloaded another independent high-coverage pooled
 102 library GM12878 replicate with 3B reads. The correlation by genomic distance in Figure 3B show
 103 slightly better correlation than the biological replicate data.
 104 We also ran HiC-DC+ (12) to call significant 3D interactions ($qvalue \leq 0.05$) on chromosome 18
 105 (Figure 3C) and obtained good overlap with interactions identified on high-resolution Hi-C data.

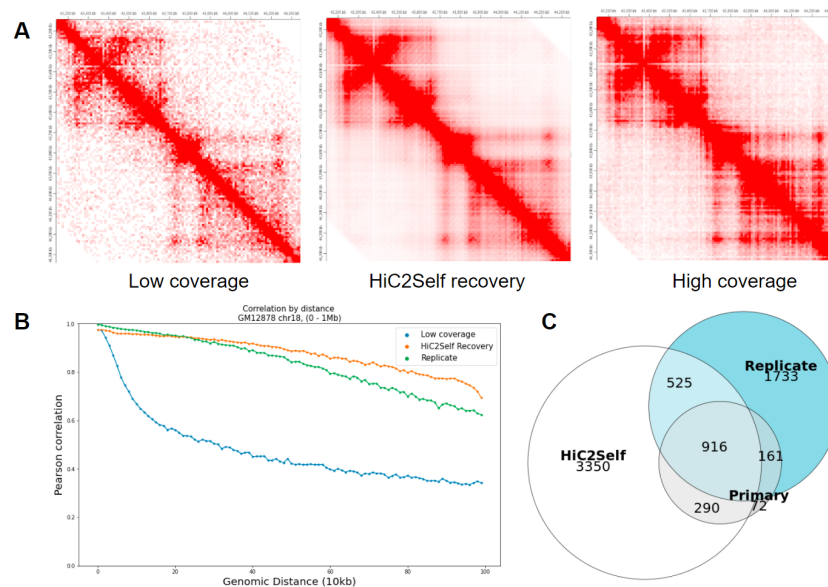


Figure 3: Performance on raw count data

106 4 Discussion

107 In this study, we developed HiC2Self, a self-supervised Hi-C contact map denoising model that
 108 achieves comparable performance with supervised Hi-C denoising methods without the requirement
 109 to train on paired low- and high-coverage data sets. Importantly, the model trains on unnormalized
 110 raw count data and produces high-coverage contact maps in count space, facilitating downstream
 111 analyses using Hi-C tools such as TAD and interaction callers.

112 We compared HiC2Self (with necessary changes) with existing supervised methods for denoising
 113 normalized Hi-C contact matrices and also assessed the usefulness of denoised read count contact
 114 matrices for downstream analyses. Interestingly, we found that adding SVD reconstructions of
 115 low-coverage matrices as input channels led to improved performance, and indeed our self-supervised
 116 model was competitive with a state-of-the-art supervised denoising method. Potentially our SVD
 117 reconstruction channels might improve supervised approaches as well. In additional experiments
 118 (not described above), we found that the generalizability of supervised models depended strongly on
 119 matching the low-/high sequencing coverage relationship in training data to the test data. A mismatch
 120 between training and test sequencing coverage scenarios led to poor performance, suggesting some
 121 inflexibility in the model for generalization. Our self-supervised model avoids this challenge of
 122 generalization and showed robust performance across data sets. In the raw count space comparison,
 123 our model recovered a majority of the significant interactions identified by high-resolution Hi-C data,
 124 showing its capacity as a valid denoising tool for downstream analysis. We will continue working on
 125 the evaluation of model performance and analysis of results in future work.

References

- 126
- 127 [1] Szabo, Q., Bantignies, F., Cavalli, G., et al. Principles of genome folding into topologically
128 associating domains. *Science Advances*. 2019;5(4):eaaw1668. doi:10.1126/sciadv.aaw1668
- 129 [2] Zhang, Y., An, L., Xu, J., et al. Enhancing Hi-C data resolution with deep convolutional neural
130 network HiCPlus. *Nature Communications*. 2018;9:750. doi:10.1038/s41467-018-03113-2
- 131 [3] Liu, T., Wang, Z., et al. HiCNN: a very deep convolutional neural network to
132 better enhance the resolution of Hi-C data. *Bioinformatics*. 2019;35(21):4222-4228.
133 doi:10.1093/bioinformatics/btz251
- 134 [4] Liu, Q., Lv, H., Jiang, R. hicGAN infers super resolution Hi-C data with generative adversarial
135 networks. *Bioinformatics*. 2019;35(14):i99-i107. doi:10.1093/bioinformatics/btz317
- 136 [5] Hong, H., Jiang, S., Li, H., et al. DeepHiC: A generative adversarial network for
137 enhancing Hi-C data resolution. *PLoS Computational Biology*. 2020;16(2):e1007287.
138 doi:10.1371/journal.pcbi.1007287
- 139 [6] Dimmick, M., Lee, L., Frey, B. HiCSR: a Hi-C super-resolution framework for producing highly
140 realistic contact maps. *bioRxiv - Genomics*. 2020. doi:10.1101/2020.02.24.961714
- 141 [7] Batson, J., Royer, L. Noise2Self: Blind Denoising by Self-Supervision. *arXiv - cs.CV*.
142 2019;1901.11365. arXiv:1901.11365
- 143 [8] Eraslan, G., Simon, L.M., Mircea, M. et al. Single-cell RNA-seq denoising using a deep count
144 autoencoder. *Nature Communications*. 2019;10(390). doi:10.1038/s41467-018-07931-2
- 145 [9] Durand, N., Shamim, M., Machol, I., et al. Juicer provides a one-click system for analyzing loop-
146 resolution Hi-C experiments. *Cell Systems*. 2016;3(1):95-98. doi:10.1016/j.cels.2016.07.002
- 147 [10] Rao, S., Huntley, M., Durand, N., et al. A 3D map of the human genome at kilo-
148 base resolution reveals principles of chromatin looping. *Cell*. 2014;159(7):1665-80. doi:
149 10.1016/j.cell.2014.11.021
- 150 [11] Larsson, J. eulerr: Area-Proportional Euler and Venn Diagrams with Ellipses. R package. 2020.
- 151 [12] Sahin, M., Wong, W., Zhan, Y., Van Deynze, K., Koche, R., Leslie, C.S. HiC-DC+: systematic
152 3D interaction calls and differential analysis for Hi-C and HiChIP. In preparation.